Supporting Information

Edeling et al. 10.1073/pnas.1322036111

SI Experimental Procedures

Nonstructural Protein 1 Expression and Purification. A West Nile virus nonstructural protein 1 (WNV NS1) C-terminal construct (residues 172–352) was cloned into the NheI and NotI restriction sites of pET21a for expression in the BL21 (DE3) codon plus *Escherichia coli* cells by autoinduction (1). Inclusion bodies (200–300 mg), isolated using established methods (2), were denatured in 7 M guanidinium hydrochloride and 30 mM β-mercapthanol for 1 h at 37 °C, centrifuged for 10 min at 4 °C, and diluted to 2 M guanidinium hydrocloride in 50 mM sodium acetate pH 5.2. The supernatant was filtered and refolded by rapid, serial dilution (1-mL injections, hourly) in 1 L of refolding buffer (400 mM L-arginine, 100 mM Tris-base pH 8.3, 2 mM EDTA, 0.5 mM oxidized glutathione, 5 mM reduced glutathione, and 0.2 mM phenylmethanesulfonyl fluoride) at 4 °C. The recombinant protein was concentrated using a stirred cell concentrator with YM10 membrane (Millipore), centrifuged to remove aggregates and purified on an S-75 size-exclusion chromatography (SEC) column equilibrated in 20 mM Hepes pH 7.4 and 150 mM NaCl, buffer A. NS1 protein eluates were buffer exchanged into 50 mM bis·Tris propane pH 9.5 and 10 mM NaCl and then loaded onto an ion-exchange mono Q 5/50 column. A salt gradient (10–400 mM NaCl) was applied to elute NS1, which was again purified by S-75 SEC.

$NS1_{172–352}$ Crystal Structure Determination. We produced milligram quantities of purified, full-length recombinant WNV and Dengue virus (DENV) (serotype 1, DENV-1) proteins in insect cells and bacteria. In our experiments, WNV and DENV NS1 proteins produced in the supernatant of Hi-5 insect cells yielded needle-like crystals that never diffracted beyond 10 Å. N-terminal sequencing of a stable fragment of WNV NS1 produced in bacteria revealed a sequence of V-R-E-S, which corresponded to amino acids 171–174. Amino acid residues R172–A352 were cloned, expressed, and purified and migrated as a single homogeneous band on SDS/PAGE. The protein was concentrated to ∼8 mg/mL and crystallized by hanging-drop vapor diffusion in 20% (wt/vol) PEG 2K MME, 0.1 M sodium acetate pH 5.4. The crystals were optimized by streak seeding and cryo-protected in 22% (wt/vol) PEG 2K MME, 0.1 M sodium acetate pH 5.4, 25% (wt/vol) glycerol. Initial attempts to phase selenomethionine-labeled protein crystals by single-wavelength anomalous diffraction were unsuccessful, likely because of the low methionine content (0.5%) of this fragment. Sequence alignment of NS1 homologs revealed residues that might tolerate methionine substitution. WNV NS1 was engineered to express two mutations (I184M + L241M) from which single-wavelength anomalous diffraction phasing was successful.

A wavelength scan of these crystals on the Advanced Light Source (ALS) beamline 4.2.2 (Lawrence Berkeley Laboratories) revealed the peak at 12664.4 keV and inflection at 12661.3 keV. Data were collected at the peak wavelength at 100 K and indexed and scaled with Mosflm and SCALA, respectively. Autosharp identified three of the five selenomethionine residues, and the phase maps were improved by density modification and solvent flattening to 54%. Automated model building in Arpwarp successfully built 149 residues with R_{factor} 21.6% and R_{free} 30.5%. Model building was performed in Coot and refinement in Refmac or Phenix. The final model was refined to 1.85 Å resolution and belonged to the space group $P3_121$ with unit cell dimensions of $a = b = 49.71$ Å, $c = 139.85$ Å, and $\alpha = \beta = 90°$, $\gamma = 120°$ with one copy of $NS1_{172–352}$ per asymmetric unit. Data collection and refinement statistics are reported in Table S1.

DENV-1 $NS1_{172–352}$ was produced in a manner similar to WNV $NS1_{172–352}$ and crystallized at 12 mg/mL in 20% (wt/vol) PEG 4K, 0.2 M magnesium sulfate and 10% glycerol. Crystallographic phasing of DENV-1 $NS1_{172–352}$ was obtained by molecular replacement using Phaser (3). Crystallographic phasing of WNV $NS1_{172–352}$ in complex with 22NS1 Fab fragments was accomplished using Phaser with settings to search for two copies of WNV $NS1_{172–352}$ and either one or two copies each of Fab variable and constant domains (CTM01 IgG, PDB ID code 1AD9, as template). Inspection and refinement of the model revealed the presence of two Fab molecules in the asymmetric unit.

Complex Formation of 22NS1 Fab-WNV NS1. The 22NS1 Fab fragments were prepared by papain digestion of 10 mg of 22NS1 MAb (4) for ∼18 h at 37 °C as per the manufacturer's instructions (Pierce). Following protein A agarose affinity chromatography to remove Fc fragments and undigested MAb, Fab fragments were purified further on an S-75 SEC column. Purified 22NS1 Fab was mixed with excess WNV $NS1_{172–352}$ and the complex was isolated for crystallization after SEC and crystallized by hanging-drop vapor diffusion at 9 mg/mL in 8% PEG 8 K and 0.1 M sodium citrate.

SEC Multiangle Light Scattering. The oligomeric state of WNV and DENV-1 $NS1_{172–352}$ in solution was determined by SEC multi-angle light scattering (MALS) after injecting 100 μL of 3–8 mg/mL purified protein onto an S-75 SEC in line with a Dawn HELEOS-II 18-angle light-scattering detector (Wyatt), Optilab rEX refractive index monitor (Wyatt), and Waters HPLC system. Data analysis was performed with Astra V software (Wyatt).

Small-Angle X-Ray Scattering. Small-angle X-ray scattering (SAXS) data were collected at the ALS SIBYLS beamline 12.3.1. Proteins purified by SEC were loaded into a 96-well plate (Axygen Scientific) at three different concentrations (within an ∼1- to 10-mg/mL range), together with sample-matched buffers, and sealed with protected film. Scattering data were collected at four different exposures (0.5-, 1-, 6-, and a final 0.5-s exposure). Forward scattering I(0) and the radius of gyration Rg were calculated from both the Guinier and entire region of the scattering curve using the pairwise distribution function P(r), which also provides the maximum particle dimension, D_{max}. Molecular weight estimation was estimated using the SAXSMoW applet (www.if.sc.usp.br/∼saxs) (5). Data processing was performed in PRIMUS (6). For SAXS analysis of WNV $NS1_{172–352}$, experimental and predicted scattering profiles (from crystal structures) were compared using CRYSOL (6) at 3.7 mg/mL (and 7.4 mg/mL) after cropping datapoints before the Guinier region and extending out to 2.5 nm^{-1}. Rg analysis [using AutoRg in PRIMUS (6)] of samples at 1 mg/mL (26.2 ± 0.12), 3.7 mg/mL (Rg = 25.8 ± 0.32), and 7.4 mg/mL (Rg = 26.07 ± 0.12) showed no evidence of concentration dependence, where Rg is the average and SEM from each sample in the concentration series exposed for at least two of three exposures of 0.5, 1, and 6 s each, and buffer subtracted (data that showed changes in Rg of ≥ 4 Å were removed from further analysis). Ab initio envelopes were calculated from a merged short (0.5 s) and long (6 s) exposure scattering dataset at 3.7 mg/mL (total estimate of 0.67, defined as reasonable) using 10 envelope calculations with P1 symmetry in DAMMIF (6). A consensus envelope was generated using DAMAVER, which was characterized by a normal spatial discrepancy (NSD), of 0.74 ± 0.02 (where NSD represents a quantitative measure of similarity between

sets of 3D points, and NSD < 0.7 is good, 0.7–1 reasonable, >1 poor, agreement between models). Superimposition of the structure into the resulting averaged envelope was completed by SUPCOMB13 (6).

1. Studier FW (2005) Protein production by auto-induction in high density shaking cultures. *Protein Expr Purif* 41(1):207–234.
2. Shrestha B, et al. (2010) The development of therapeutic antibodies that neutralize homologous and heterologous genotypes of Dengue virus type 1. *PLoS Pathog* 6(4):e1000823.
3. McCoy AJ, et al. (2007) Phaser crystallographic software. *J Appl Cryst* 40(Pt 4):658–674.
4. Chung KM, et al. (2006) Antibodies against West Nile Virus nonstructural protein NS1 prevent lethal infection through Fc gamma receptor-dependent and -independent mechanisms. *J Virol* 80(3):1340–1351.
5. Fischer H, de Oliveira Neto M, Napolitano HB, Polikarpov I, Craievich AF (2010) Determination of the molecular weight of proteins in solution from a single small-angle X-ray scattering measurement on a relative scale. *J Appl Cryst* 43:101–109.
6. Petoukhov MV, Konarev PV, Kikhney AG, Svergun DI (2007) ATSAS 2.1 - towards automated and web-supported small-angle scattering data analysis. *J Appl Crystallogr* 40(Suppl):s223–s228. Available at http://scripts.iucr.org/cgi-bin/paper?sm6018. Accessed November 22, 2013.

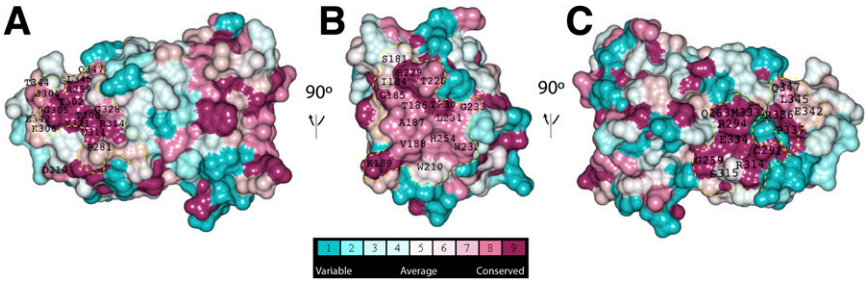

Fig. S1. (*A–C*) Three highly conserved regions on the surface of WNV $NS1_{172–352}$. Residues contributing to each highly conserved surface patch on WNV $NS1_{172–352}$ are indicated, and the surface is colored by conservation as shown in the legend below the figure (1).

1. Landau M, et al. (2005) ConSurf 2005: The projection of evolutionary conservation scores of residues on protein structures. *Nucleic Acids Res* 33(Web Server issue):W299–W302.

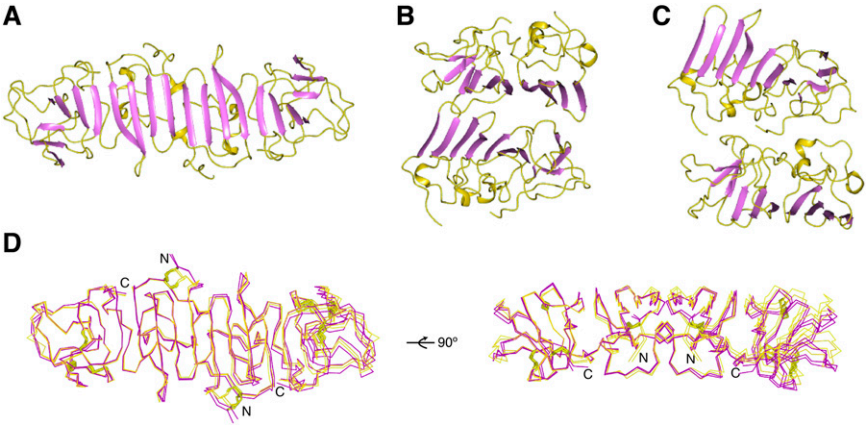

Fig. S2. The structure of WNV $NS1_{172–352}$ crystallographic dimer interfaces. (*A*) The extended β-sheet dimer, (*B*) a sandwiched β-sheet dimer arrangement, and (*C*) a dimer characterized by loop-face interactions. (*D*) C-α trace of each of the four extended β-sheet dimers [WNV $NS1_{172–352}$ in complex with 22NS1 Fab (gold) and the two DENV1 $NS1_{172–352}$ dimers present in the asymmetric unit of the crystal (purple) were overlain on one monomer of the WNV $NS1_{172–352}$ extended β-sheet dimer (light gold). The C-terminal domain dimer is a conserved rigid platform with only minor tilts at the twofold axis of symmetry.

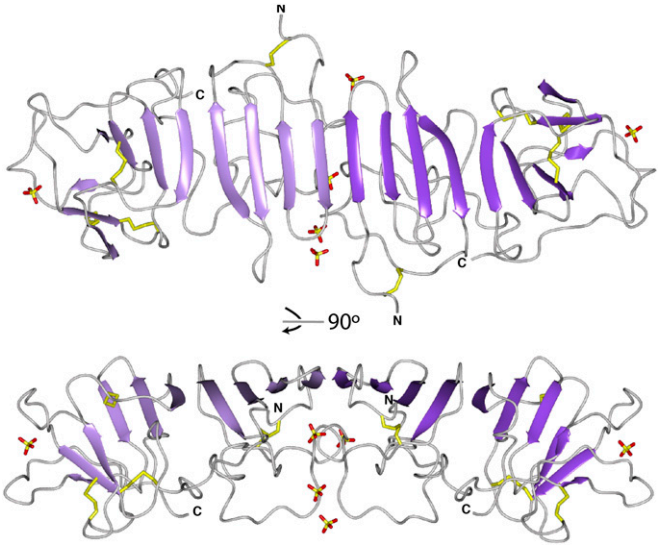

Fig. S3. Crystal structure of DENV-$1_{172–352}$. DENV-$1_{172–352}$ crystallizes with two head-to-head dimers in the asymmetric unit, which are structurally indistinguishable (rmsd of 0.496 Å in the α-carbons over 350 amino acids) and similar to dimeric WNV $NS1_{172–352}$ (rmsd of 0.98 Å in the α-carbons over 347 amino acids). A representative dimer is shown: one monomer is shaded in light purple, the other dark purple. Six sulfates (shown in cylinders) are present per DENV-$1_{172–352}$ dimer, four of which cluster at the dimer interface on the complex loop face of DENV-1 $NS1_{172–352}$, identifying an extended region (four sulfates) on the surface of NS1 for binding ligands of anionic character. The remaining two sulfates make interactions at each end of the dimer.

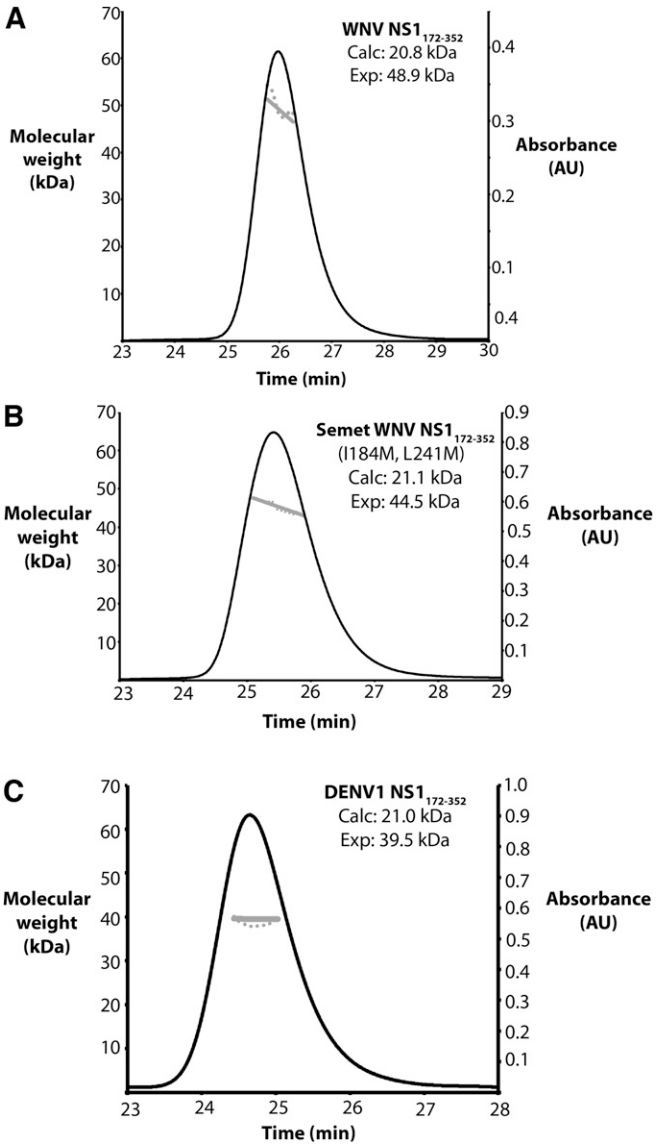

Fig. S4. WNV $NS1_{172–352}$, WNV $NS1_{172–352}$ I184M + L241M, and DENV-1 are dimers in solution. SEC-MALS analysis of (*A*) WNV $NS1_{172–352}$ and (*B*) WNV $NS1_{172–352}$, engineered to express a double mutant (I184M, L241M), which was necessary for single-wavelength anomalous diffraction phasing, and (*C*) DENV-$1_{172–352}$ reveals molecular weights that are approximately twice the theoretical molecular weights of the respective monomers.

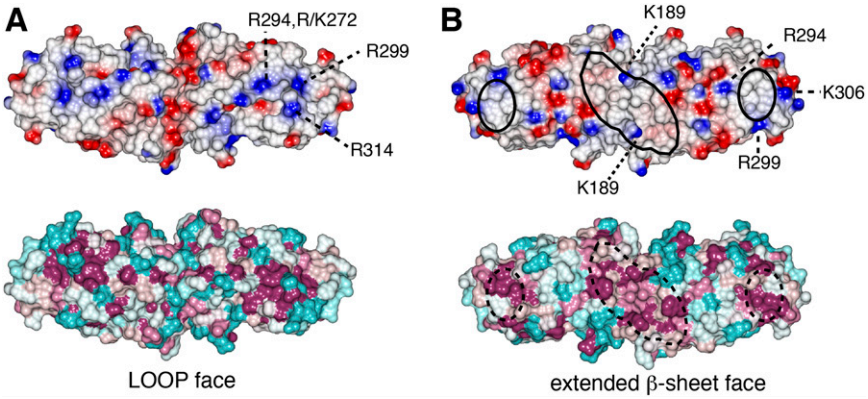

Fig. S5. Structural features of the β-platform and loop faces of $NS1_{172–352}$. Electrostatic (*Upper*) and surface conservation representation (*Lower*) of the (*A*) loop face and (*B*) extended β-sheet of dimeric $NS1_{172–352}$. Electrostatic surface is colored from −19 kT/e (red) to +19 kT/e (blue).

Table S1. WNV, DENV-1 $NS1_{172–352}$, and WNV $NS1_{172–352}$-22NS1 Fab complex crystal structure data collection and refinement statistics

Data collection and refinement statistics	WNV $NS1_{172–352}$	DENV-1 $NS1_{172–352}$	WNV $NS1_{172–352}$-22NS1 Fab
Wavelength	0.97 Å	1.00 Å	1.00 Å
Resolution	24–1.85 Å (1.95–1.85 Å)	20–2.7 Å (2.82–2.70Å)	50.0–3.0 Å (3.11–3.0 Å)
No. of observed reflections	99,510	84,535	105,869
Unique reflections	17,797	23,633	28,187
Redundancy	5.6 (6.8)	3.6 (3.4)	3.8 (3.8)
I/σI	10.5 (3.4)	12.7 (2.3)	11.6 (1.96)
R_{merge}*	9.6 (54.8)	9.6 (55.3)	12.4 (69.8)
Completeness	99.7% (100%)	100% (100%)	100% (100%)
Spacegroup	$P3_121$	C2	C2
Cell dimensions	a = 49.71 Å, b = 49.71 Å, c = 139.85 Å; α = β = 90° γ = 120°	a = 109.18 Å, b = 81.96 Å, c = 97.19 Å; α = γ = 90°, β = 97.78	a = 215.87 Å, b = 49.55 Å, c = 130.07 Å; α= γ = 90°, β = 91.21
Phasing statistics			
No. sites/no. expected	3/5		
Figure of merit after SHARP	0.195		
Figure of merit after solvent flattening	0.910		
Refinement statistics			
Resolution	24.9 Å (1.85 Å)	19.9 Å (2.7 Å)	40.8 Å (3.0 Å)
No. of reflections/No. in R_{free}	17,749/903	123,414/1,171	28,183/1,428
R_{cryst}/R_{free}†	20.1%/25.2%	20.3%/25.8%	21.8%/26.3%
Rmsd bond lengths	0.004Å	0.005Å	0.003Å
Rmsd bond angles	0.884°	1.181°	0.738°
PDB ID	4OIE	4OIG	4OII

Numbers in parentheses refer to the highest resolution shell.
*$R_{merge} = \Sigma|I - \langle I\rangle|/\Sigma\langle I\rangle$, where I is the intensity of each individual reflection.
†$R = \sum(F_P - F_{calc})/\sum F_P$.

Table S2. Dimer interface analysis of $NS1_{172–352}$

$NS1_{172–352}$ crystal form	Buried surface area (Å^2)*	Total buried surface area (Å^2)	Hydrogen bonds	Salt bridges	Long axis (nm)†	SAXS fit (χ^2)‡
WNV $NS1_{172–352}$						
1§	731	1,463	8	0	9.9	1.7
2	693	1,386	10	4	7.2	5.22
3	510	1,020	9	2	8.1	3.4
WNV NS1 + 22NS1 Fab						
1§	745	1,490	13	0	10.3	1.7
2	648	1,296	2	4	6.7	5.6
DENV1 NS1¶						
1§	846	1,692	17	2	9.9	1.6
2	663	1,326	4	0	8.2	2.8
3	533	1,066	6	0	7.5	4.3
4	517	1,034	2	23	9.4	1.9
5	323	646	0	1	9.4	1.8
DENV1 NS1‖						
1§	836	1,672	17	2	9.9	1.6
2	761	1,522	5	0	8.2	2.9

*Only interfaces that bury more than 110 Å^2 are shown and are defined by PISA (1).
†Long axis of the crystal dimer calculated by Crysol (2). The long axis (D_{max}) calculated from the experimental SAXS scattering profile is 9 nm.
‡Fit of the calculated scattering profile from the crystal structure to the experimental scattering profile using the program Crysol (2).
§The dimer with the greatest buried surface area provides the best fit to the SAXS solution data and is the extended β-sheet dimer.
¶DENV1 NS1 noncrystallographic dimer 1.
‖DENV1 NS1 noncrystallographic dimer 2.

1. Krissinel E, Henrick K (2007) Inference of macromolecular assemblies from crystalline state. *J Mol Biol* 372(3):774–797.
2. Petoukhov MV, Konarev PV, Kikhney AG, Svergun DI (2007) ATSAS 2.1 - towards automated and web-supported small-angle scattering data analysis. *J Appl Crystallogr* 40(Suppl): s223–s228. Available at http://scripts.iucr.org/cgi-bin/paper?sm6018. Accessed November 22, 2013.

Table S3. Residues in WNV $NS1_{172–352}$ dimer interface

Number	Residue	ASA (Å^2)	BSA (Å^2)	ΔG* (kcal/mol)	Conservation†
1	S181	49.53	5.22	−0.06	Conserved
2	K182	161.52	17.06	−0.19	Variable
3	I183	108.24	11.38	0.18	Conserved
4	I184	25.43	23.34	−0.20	Conserved
5	G185	36.68	21.70	0.34	Highly conserved
6	T186	37.33	36.61	−0.22	Highly conserved
7	A187	60.61	23.19	0.37	Highly conserved
8	V188	67.37	66.83	0.46	Conserved
9	K189	146.33	34.31	−0.12	Highly conserved
10	N190	124.87	27.41	−0.27	Conserved
11	N191	81.52	1.90	−0.20	Variable
12	L206	70.40	2.84	0.05	Variable
13	W210	67.49	35.08	0.27	Conserved
14	E227	93.57	58.61	0.31	Variable
15	T228	120.86	100.40	0.74	Conserved
16	H229	52.22	49.43	−0.01	Highly conserved
17	T230	20.92	20.81	−0.21	Highly conserved
18	L231	45.08	45.08	0.72	Conserved
19	W232	100.55	59.69	0.41	Conserved
20	G233	31.24	26.79	−0.08	Conserved
21	D234	102.12	54.5	0.39	Variable
22	H254	12	10.13	0.83	Highly conserved

*Predicted by assembly analysis in the program PISA (1).

†Conservation based on CONSURF analysis (2) scores from alignment of 53 NS1 homologs (representative alignment shown in Fig. S1*B*) and defined as highly conserved (score range of 8–9), conserved (score range of 5–7), or variable (score range of 1–4).

1. Krissinel E, Henrick K (2007) Inference of macromolecular assemblies from crystalline state. *J Mol Biol* 372(3):774–797.
2. Landau M, et al. (2005) ConSurf 2005: The projection of evolutionary conservation scores of residues on protein structures. *Nucleic Acids Res* 33(Web Server issue):W299–W302.

Table S4. Direct contacts between 22NS1 and $NS1_{172–352}$

$NS1_{172–352}$		22NS1		Distance (Å)
Van der Waals contacts*				
Trp^{232}	Cζ2	Trp^{L92}	CH2	3.38
Trp^{232}	Cz2	Trp^{L92}	Cz2	3.40
Trp^{232}	Cz2	His^{L30}	Cε1	3.66
Trp^{232}	CH2	Trp^{L92}	CH2	3.58
Gly^{235}	C	Thr^{L94}	Cγ2	3.55
Ile^{236}	C	Thr^{L94}	Cγ2	3.52
Leu^{237}	Cδ2	Thr^{L94}	Cβ	3.75
Leu^{237}	Cδ2	Arg^{L96}	Cζ	3.63
Ser^{239}	Cβ	Trp^{H33}	Cε2	3.65
Asp^{240}	Cγ	Tyr^{H98}	Cε1	3.54
Asn^{253}	Cβ	Trp^{L92}	Cζ2	3.78
Asn^{253}	Cβ	Trp^{L92}	CH2	3.55
Asn^{253}	Cγ	Trp^{L92}	Cζ2	3.43
Asn^{253}	Cγ	Trp^{L92}	CH2	3.68
Tyr^{260}	C	Try^{H98}	Cε2	3.66
Lys^{261}	Cδ	Tyr^{H98}	Cζ	3.74
Lys^{261}	Cε	Asp^{H95}	Cγ	3.54
Lys^{261}	Cε	Tyr^{H98}	Cδ1	3.85
Lys^{261}	Cε	Tyr^{H98}	Cε1	3.67
Lys^{261}	Cε	Tyr^{H98}	Cζ	3.78
Thr^{262}	Cγ2	Trp^{H33}	Cζ2	3.81
Thr^{262}	Cγ2	Trp^{H33}	CH2	3.57
His^{293}	Cβ	Tyr^{H332}	Cζ	3.87
His^{293}	Cδ2	Tyr^{H32}	Cα	3.88
His^{293}	Cδ2	Tyr^{H32}	Cβ	3.33
Arg^{294}	Cβ	Ser^{H31}	Cβ	3.38
Ser^{315}	Cβ	Gly^{H97}	Cα	3.77
Electrostatic interactions†				
Lys^{261}	Nζ	Asp^{H95}	NH2	2.86
Glu^{289}	Oε1	Arg^{H99}	NH2	3.92
Arg^{314}	NH1	Asp^{H96}	Oδ2	3.14
Arg^{314}	NH2	Asp^{H96}	Oδ2	3.68
Asp^{240}	Oδ1	Arg^{L96}	NH2	3.24
Asp^{240}	Oδ2	Arg^{L96}	NH1	3.34
Asp^{240}	Oδ2	Arg^{L96}	NH2	2.85
Direct hydrogen bonds‡				
Gly^{235}	O	Thr^{L94}	N	3.13
Asp^{240}	Oδ2	Arg^{L96}	NH1	3.34
Asp^{240}	Oδ2	Arg^{L96}	NH2	2.85
Tyr^{260}	O	Tyr^{H98}	OH	2.64
Lys^{261}	Nζ	Asp^{H95}	Oδ2	2.86
Arg^{314}	NH1	Asp^{H96}	Oδ2	3.14
Ser^{315}	Oγ	Asp^{H96}	O	2.57
Asn^{351}	Nδ2	Asn^{H53B}	Oδ1	2.62

*Van der Waals interactions defined in Ligplot (1).
†Electrostatic interactions as defined by PISA (2).
‡Hydrogen bonds as defined by HBPLUS (3) in Ligplot.

1. Wallace AC, Laskowski RA, Thornton JM (1995) LIGPLOT: A program to generate schematic diagrams of protein-ligand interactions. *Protein Eng* 8(2):127–134.
2. Krissinel E, Henrick K (2007) Inference of macromolecular assemblies from crystalline state. *J Mol Biol* 372(3):774–797.
3. McDonald IK, Thornton JM (1994) Satisfying hydrogen bonding potential in proteins. *J Mol Biol* 238(5):777–793.